

Intrinsic Electric Fields in Ionic Liquids Determined by Vibrational Stark Effect Spectroscopy and Molecular Dynamics Simulation

Shiguo Zhang,^[a] Rui Shi,^[b] Xiangyuan Ma,^[a] Liujin Lu,^[a] Yude He,^[a] Xiaohu Zhang,^[b] Yanting Wang,^{*,[b]} and Youquan Deng^{*,[a]}

Ionic liquids (ILs) are salts formed by a combination of specific cations and anions, whose melting points are around room temperature.^[1] Owing to their unique properties, which are advantageous over those of conventional solvents in many aspects, ILs nowadays are very fascinating in various fields, including organic synthesis,^[1a,2] catalysis,^[3] inorganic chemistry,^[4] electrochemistry,^[5] and materials.^[6] Many chemical processes utilizing ILs demonstrate effects and outcomes very different from those obtained in molecular solvents.^[7] For instance, large increases in reactivity and selectivity have been achieved by using ILs for homogeneously catalyzed reactions,^[3a] and reactions in ILs may sometimes adopt a fundamentally different pathway from those in molecular solvents.^[8] The novel behavior was vaguely ascribed to the so-called “ionic liquid effect” or “ionic liquid environment”.^[2e,8,9] Since ILs are composed solely of ions, the intuition that ILs have much stronger electric fields than common molecular solvents has been generally accepted without careful study, and many distinctive features of ILs which distinguish them from common molecular solvents,^[10] such as low volatility, tunable solubility, good conductivity, wide electrochemical window, and distinct reactivity and selectivity to reaction, are attributed to their strong intrinsic electrostatic interactions and fields.^[5d] Therefore, determining the strength of the intrinsic electric fields in ILs is of fundamental importance to understanding the properties of ILs and to their applications. Unfortunately, until now the intrinsic electric fields in ILs have remained poorly understood, and their identification and quantification are very challenging. In this work, we evaluate for the first time the

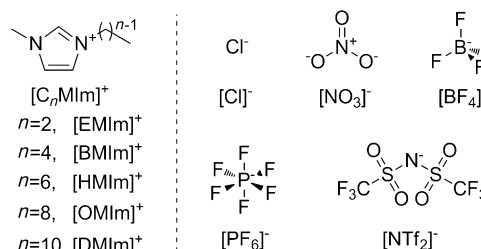


Figure 1. Structures and abbreviations of the cations and the anions being investigated.

intrinsic electric fields in a series of commonly used 1-alkyl-3-methylimidazolium ILs (Figure 1) by using vibrational Stark effect (VSE) spectroscopy along with molecular dynamics (MD) simulations. The results obtained in this study indicate that the intrinsic electric fields in ILs are only slightly higher than but still comparable to those in common molecular solvents, and are strongly structure-dependent.

VSE spectroscopy (also known as electroabsorption spectroscopy^[11]) is an experimental technique typically used to evaluate the relative electric fields between two electrostatic environments (two kinds of ILs in our case) by measuring the observed IR frequency shifts of the probe molecule,^[12]

$$\Delta \vec{E} = -\Delta \bar{\nu}_{CN}^{obs} / (\Delta \bar{\mu}_{CN} / hc) \quad (1)$$

where h is Planck's constant, c is the speed of light, $\Delta \vec{E}$ is the electric field difference on the probe, $\Delta \bar{\nu}_{CN}^{obs}$ is the observed IR frequency shift, and $\Delta \bar{\mu}_{CN}$ is the characteristic linear Stark tuning rate, a quantity that describes the sensitivity of the probe to the electric fields, which can be determined by measuring the VSE spectroscopy in a known electric field. Although VSE has been extensively used to study ordered environments, such as protein^[12c,12] and polymer matrices,^[13] in particular to understand the electrostatic environment within the idiosyncratic interior of folded proteins and its connection to biomolecular functions,^[12c,12] only very recently did Boxer et al.^[14] successfully extend the VSE method to homogeneous systems, such as molecular solvents. They determined a range of electric fields for molecular solvents, including protic and aprotic solvents, by studying the relation between the IR frequency shift $\nu_{C\equiv N}$ and the ^{13}C NMR chemical shift $\delta(^{13}CN)$ of ethyl thiocyanate

[a] S. Zhang,* X. Ma, L. Lu, Y. He, Prof. Y. Deng
Center for Green Chemistry and Catalysis
Lanzhou Institute of Chemical Physics, Chinese Academy of Sciences
Lanzhou 730000 (P. R. China)
Fax: (+86)931-4968-141
E-mail: ydeng@licp.cas.cn

[b] R. Shi,* X. Zhang, Prof. Y. Wang
Key Laboratory of Frontiers in Theoretical Physics
Institute of Theoretical Physics and Kavli Institute for Theoretical
Physics China
Chinese Academy of Sciences, Beijing 100190 (P. R. China)
Fax: (+86)10-6256-2587
E-mail: wangyt@itp.ac.cn

[*] These authors contributed equally to this work.

Supporting information for this article is available on the WWW
under <http://dx.doi.org/10.1002/chem.201201257>.

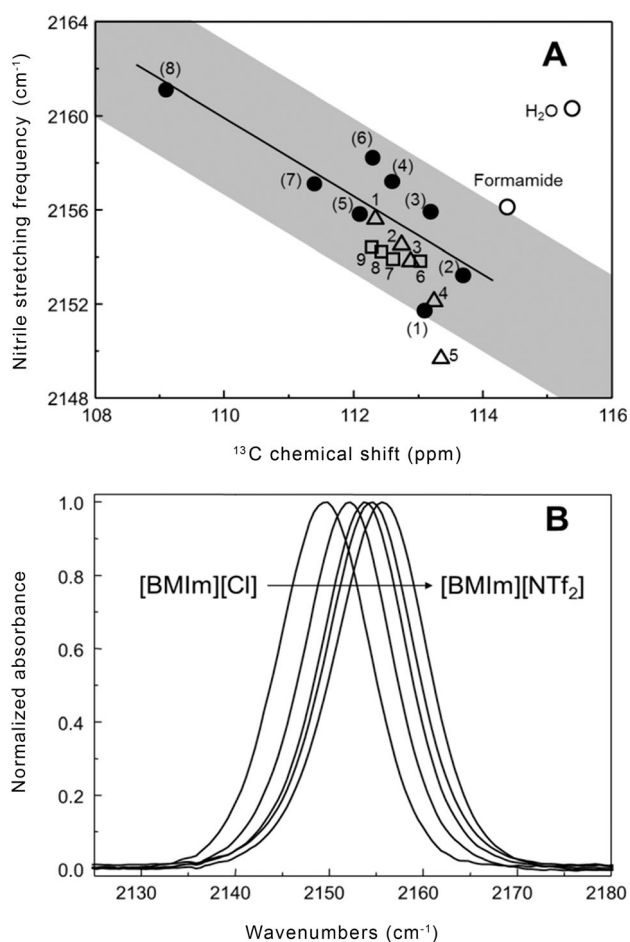


Figure 2. A) Nitrile stretching frequencies $\nu_{\text{C}\equiv\text{N}}$ versus ^{13}C chemical shifts $\delta(^{13}\text{C})$ in ILs and molecular solvents (data of molecular solvents were from ref. [14]). Molecular solvents (●): (1) DMSO, (2) DMF, (3) acetone, (4) CD_2Cl_2 , (5) THF, (6) CDCl_3 , (7) toluene, (8) cyclohexane. [BMIm][X] ILs (Δ): 1-[BMIm][NTf₂], 2-[BMIm][PF₆], 3-[BMIm][BF₄], 4-[BMIm][NO₃], 5-[BMIm][Cl]. [C_nMIm][BF₄] ILs (\square): 6-[EMIm][BF₄], 7-[HMIm][BF₄], 8-[OMIm][BF₄], 9-[DMIm][BF₄]. The black line indicates the best fit for the $\nu_{\text{C}\equiv\text{N}}$ versus ^{13}C NMR data of molecular solvents excluding H-bonding solvents.^[14] B) Normalized IR absorption spectra of $\nu_{\text{C}\equiv\text{N}}$ in [BMIm]-based ILs (from left to right: [Cl], [NO₃], [BF₄], [PF₆], and [NTf₂], respectively).

(EtSCN, $0.72 \text{ cm}^{-1}/(\text{MV cm}^{-1})$), the probe used in their experiments. More specifically, as shown in Figure 2A, if the data point for one solvent locates in the range of the confidence interval marked in gray (e.g. DMSO, DMF, acetone, CD_2Cl_2 , THF, CDCl_3 , toluene, or cyclohexane), the observed IR shift in this solvent can be attributed to the change in the local electric field, and thus $\Delta\vec{E}$ can be directly determined from $\Delta\bar{\nu}_{\text{CN}}^{\text{obs}}$. On the other hand, if the data point locates above the confidence interval (e.g. formamide and water), the IR shift should be decomposed into electrostatic and H-bonding contributions, respectively, and $\Delta\vec{E}$ is determined by subtracting the displacement caused by H-bonding from $\Delta\bar{\nu}_{\text{CN}}^{\text{obs}}$.

In our experiments, we also use EtSCN as the IR probe since it provides an optimal combination of oscillator

strength, frequency, and Stark tuning rate for measurements in biological systems and organic solvents.^[14,15] The measured $\nu_{\text{C}\equiv\text{N}}$ frequency shift versus ^{13}C NMR chemical shift for EtSCN in various ILs are compared with the data for molecular solvents in Figure 2A (data are listed in Table S1 in the Supporting Information). Clearly, the data points for nearly all investigated ILs, except [BMIm][Cl], locate inside the confidence interval, similar to the case for aprotic molecular solvents. Although generally the ILs had been reported to be H-bonding donors due to the acidic hydrogen on the imidazolium ring,^[16] no strong H-bonding signals were observed in our experiments. Therefore, the IR shifts in ILs arise principally from electrostatic effects, and thus the corresponding relative electric field strengths can be directly calculated according to Equation (1). Moreover, the data points below the solid black line in Figure 2, which is the best fit for the $\nu_{\text{C}\equiv\text{N}}$ versus ^{13}C NMR data of aprotic molecular solvents, indicate that these ILs have slightly stronger electric fields and weaker H-bonds than molecular solvents. Nevertheless, the electric fields of most ILs still fall in the range of common molecular solvents between THF and DMSO. This experimental observation is contradictory to the widely accepted intuition that ILs should have much stronger intrinsic electric fields than molecular solvents. As described in detail in the Supporting Information, we have employed some simplified models (see Table S2) to demonstrate that, compared with inorganic salts, the surprisingly weaker than expected electric fields in ILs may be attributed to their steric and bulky ions, which effectively increase the distances between ions and thus significantly weaken the electric fields in ILs. On the other hand, although the molecules in polar molecular solvents are charge neutral, the large molecular dipole moments and short distances between dipoles still allow them to have intrinsic electric fields comparable to those in ILs. The corresponding-states surface tension calculations performed by Weiss et al.^[17] also found that ILs have physical properties more similar to molecular solvents than inorganic molten salts. Note that [BMIm][Cl] exhibits a much lower $\nu_{\text{C}\equiv\text{N}}$ vibrational frequency than any other ILs as well as molecular solvents and thus has the strongest electric field. This may be attributed to the very small anion of [BMIm][Cl], which will be rationalized below.

The relative electric fields in all ILs, taking [BMIm][Cl] as a reference, measured by the VSE experiments are listed in Table 1. The normalized IR absorption spectra of the $\nu_{\text{C}\equiv\text{N}}$ vibrational frequency for the 1-butyl-3-methylimidazolium ([BMIm][X], X = Cl, NO₃, BF₄, PF₆, or NTf₂) ILs are shown in Figure 2B. According to Equation (1), the monotonic increase of the vibrational frequency with anion size (listed in Table S3 in the Supporting Information) indicates the decrease of electric fields. For instance, [BMIm][NTf₂] has a peak position (2155.6 cm^{-1} , as listed in Table S1 in the Supporting Information) 6 cm^{-1} higher than [BMIm][Cl], corresponding to a 8.3 MV cm^{-1} decrease of the electric field. As the anion size increases, a larger separation of ions due to the enlarged volume of anions rather than higher charge de-

Table 1. Relative electric fields in ILs determined by the VSE experiments and the MD simulations.

Head ^[a]	$\Delta E_{\text{VSE}}^{\text{[a]}}$	$\Delta E_{\text{cation}}^{\text{[b]}}$	$\Delta E_{\text{anion}}^{\text{[c]}}$	$\Delta E_{\text{head}}^{\text{[d]}}$	$\Delta E_{\text{tail}}^{\text{[e]}}$
[BMIm][NTf ₂]	-8.3	-9.4	-3.7	-11.0	-7.6
[BMIm][PF ₆]	-6.8	-8.6	-7.5	-10.0	-3.6
[BMIm][BF ₄]	-5.8	-5.6	-4.6	-6.6	-2.4
[BMIm][NO ₃]	-3.5	-3.1	-3.0	-3.6	-0.8
[BMIm][Cl]	0	0	0	0	0
[EMIm][BF ₄]	-5.8	-5.7	-4.8	-7.5	1.4
[HMIm][BF ₄]	-6.0	-4.9	-3.3	-6.0	-4.5
[OMIm][BF ₄]	-6.4	-3.8	-2.6	-4.8	-6.8
[DMIm][BF ₄]	-6.7	-3.5	-1.3	-4.5	-8.8

[a] Relative electric fields in MV cm⁻¹ compared to [BMIm][Cl], determined by the VSE measurements. [b–e] Relative electric fields in MV cm⁻¹ experienced by the cations, anions, headgroups, and tail carbon atoms, respectively, compared to [BMIm][Cl], determined by the MD simulations.

localization results in the monotonical increase of the relative electric fields. The schematic illustration of this explanation based on a simplified ion pair model is given in the Supporting Information (see Table S2). Compared to the change associated with the anion species, the change of the electric field associated with the cationic alkyl chain length is much milder, as can be seen from the data listed in Table 1 for the 1-alkyl-3-methylimidazolium tetrafluoroborate ([C_nMIm][BF₄], *n* = 2, 4, 6, 8, or 10) ILs. The measured electric field is smaller for a longer-chain system and only decreases by about 0.9 MV cm⁻¹ from ethyl to decyl.

All-atom MD simulations were performed to help understand the experimental results in depth and to provide a detailed mechanism of the structure-dependence of the intrinsic electric fields in ILs. Specifically, we calculated the absolute values of the electric field strengths experienced by the cation, anion, cationic headgroup (including the imidazolium ring and the methyl and CH₂ groups attached to the ring), and the cationic tail carbon (see Figure 3). Since the electric

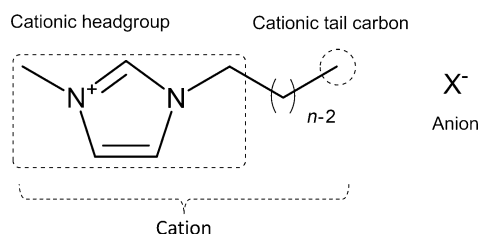


Figure 3. Definitions of cation, anion, cationic headgroup, and cationic tail carbon for the imidazolium ILs.

field at the tail CH₃ group is difficult to determine accurately due to the tiny partial charge on this group, we instead calculated the electric field at the tail carbon atom. The electric fields at the cations, anions, headgroups, and tail carbons of [BMIm][Cl] were calculated to be 26.3, 24.9, 30.6, and 32.8 MV cm⁻¹, respectively. It is clear that both the local electric fields on the headgroup and the tail carbon are larger than that experienced by the whole cation, because

the local electric fields on the subunits of the cation cancel each other and thus the net electric field on the cation is smaller than that at each subunit. Note that the electric field on the tail carbon is slightly larger than that on the headgroup, despite the fact that the positive charge of the cation is mainly located on the headgroup. This is because the strong electric fields on the individual atoms of the headgroup cancel each other and the whole headgroup exhibits a weaker electric field, which can be manifested by the very strong electric fields of 61.2 and 102.8 MV cm⁻¹, respectively, experienced by the methyl carbon and the acidic C-2 hydrogen in the headgroup of [BMIm][Cl]. The calculated relative electric fields in all ILs with respect to [BMIm][Cl] are summarized in Table 1. All the electric fields are in the order of tens of MV cm⁻¹, consistent with our previous simulation work,^[18] demonstrating that the spatial heterogeneous structure of ILs may be destroyed only when an external electric field larger than 10 MV cm⁻¹ is applied.

To visualize the change of intrinsic electric fields with IL species, the data listed in Table 1 are also plotted in Figure 4. As shown in Figure 4A, both experimental and

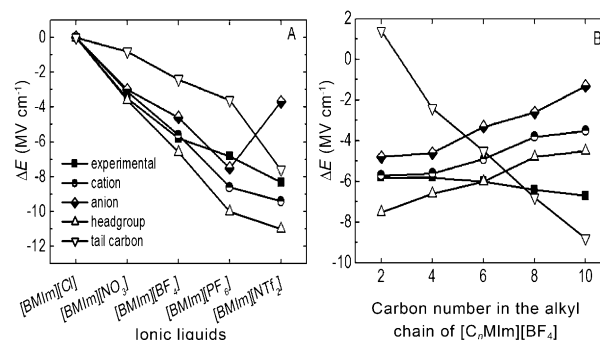


Figure 4. Relative electric fields of A) [BMIm][X] ILs and B) [C_nMIm][BF₄] ILs determined by the VSE Experiments and the MD simulations for the cations, anions, cationic headgroups, and cationic tail carbon atoms, respectively.

simulation data indicate that, except for the [NTf₂] anion, the electric fields of [BMIm][X] ILs experienced by the cations, anions, headgroups, and tail carbons all decrease monotonically with anion size. The deviation of the [NTf₂] anion from the tendency of the other anions may be explained as follows. For a symmetric anion, the local electric fields on its different subunits are partially cancelled out due to the symmetry, so the net electric field on the whole anion is relatively small. For an asymmetric anion, such as [NTf₂], the local electric fields on its subunits are very different, so the net electric field on the whole anion is larger than the symmetric ones. The structures of ILs with different anions were quantified by applying center-of-mass radial distribution functions (RDFs) between the headgroup and anion (Figure 5A). The RDFs clearly show that the average distance in the first coordination shell between the headgroups and the anions increases with anion size. As illustrated in the Supporting Information by the simplified model

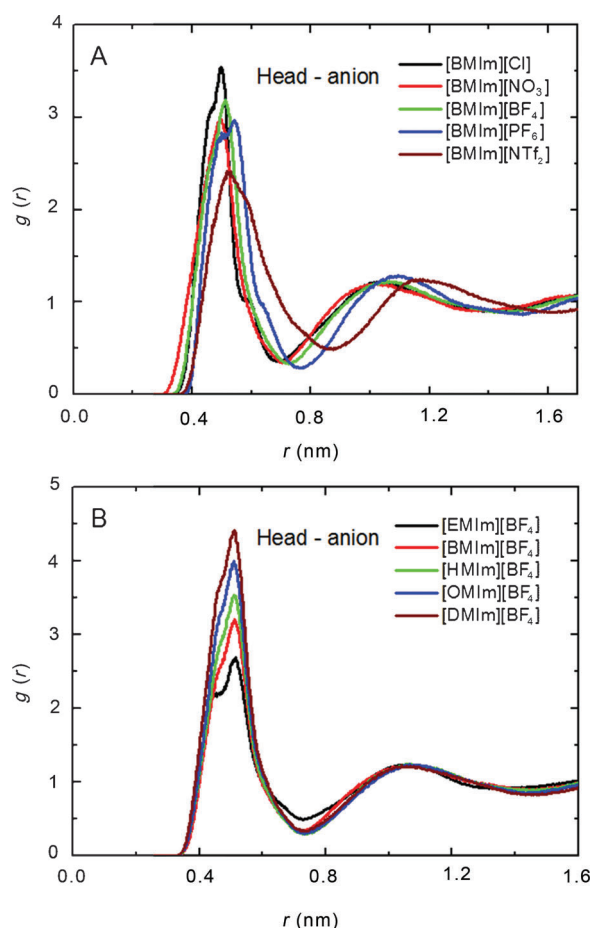


Figure 5. Center-of-mass radial distribution functions between the cationic headgroups and the anions for the IL systems with A) different anions and B) various alkyl chain lengths, respectively.

(see Table S2), this attenuates the electric fields in ILs, consistent with our experimental observation that larger anions result in weaker electric fields.

For the $[C_n\text{MIm}][\text{BF}_4]$ systems, the electric fields determined by MD simulations on the cations, anions, and headgroups increase with alkyl chain length, whereas the electric fields on the tail carbon atoms become weaker. As can be seen from Table 1 and Figure 4B, $[C_n\text{MIm}][\text{BF}_4]$ can be classified into two groups according to the calculated electric fields: 1) both experiment and simulation gave almost the same electric fields on cation and anion for $[\text{EMIm}][\text{BF}_4]$ and $[\text{BMIm}][\text{BF}_4]$, because ILs with short chains are spatially homogeneous and thus the probe in the experiment can effectively detect the electric fields on the cations and the anions; 2) as the alkyl chain elongates ($n > 4$), only the electric fields on the cationic tail carbon atoms decrease, consistent with the VSE results, but the electric fields on the cations, anions, and headgroups increase. To understand the trend for the second group, the center-of-mass RDFs between the headgroups and the anions for ILs with various alkyl chain lengths were calculated (see Figure 5B). As already shown for IL systems with long cationic side chains, the alkyl side chains aggregate and form separated nonpolar

tail domains, whereas the cationic headgroups and anions form a continuous polar network.^[19] With increasing side-chain length, the nonpolar tail domains become larger, and the cationic headgroups and anions are pushed by the tail domains to appear more at the most probable relative positions, which is demonstrated by the monotonically increasing height of the first peak with side-chain length (see Figure 5B). Therefore, the electric field in the polar domain is strengthened for a longer-chain IL system. At the same time, the electric field in the nonpolar region decreases because the average distance between the tail groups and the polar network increases. The trend determined by the VSE experiment that a longer-chain IL has a slightly weaker electric field is qualitatively consistent with the MD simulation results in the tail domain, and is very likely attributed to the fact that the probe is charge neutral, so most of the time it is away from the polar network and stays in the nonpolar tail domains.^[20] Note that our simulations were aimed to understand the intrinsic electric fields in different parts of ILs, therefore no probe molecules were simulated. A more quantitative and direct comparison between the experiment and simulation results can be made only when simulations with an explicit probe molecule are done. Such simulations will form the basis of future work.

In conclusion, for the first time, we have successfully applied the VSE spectroscopy technique to measuring the intrinsic electric fields in ILs, and have carried out an evaluation of the results by performing MD simulations. Our experimental results demonstrate that most ILs have only slightly stronger electric fields than the common molecular solvents. Both VSE spectroscopy experiments and MD simulations have revealed that the electric fields in ILs with a fixed cation apparently decrease with anion size because of the increasing distance between ions. On the other hand, with a fixed anion, the MD simulation results demonstrate that the electric fields in the polar domain are strengthened as the alkyl chain elongates, which may be attributed to the fact that the charged groups are pushed by the tail domain to statistically come closer. However, both the VSE experiments and the MD simulations indicate that the electric fields in nonpolar cationic tail domains decrease with alkyl chain length, which may be attributed to the enlarged spatial heterogeneity in ILs. The comparison of VSE and MD results suggests that, for ILs with long alkyl chains ($n > 4$), the ionic environment in ILs becomes spatially heterogeneous and thus the charge neutral probe prefers to stay in the nonpolar tail domains. Therefore, the VSE measurements are consistent with the MD simulation results in tail domain. This work provides a systematic way to evaluate the ionic environment and the intrinsic electric fields in ILs and improves our understanding of the ionic nature of ILs.

Acknowledgements

This work was supported by the National Natural Science Foundation of China (No. 21103208, 21173240 and 10974208) and the Hundred Talent

Program of the Chinese Academy of Sciences (CAS). The authors thank the Supercomputing Center in the Computer Network Information Center at the CAS for allocations of computer time.

Keywords: intrinsic electric fields • ionic liquids • molecular dynamics simulation • vibrational Stark effect

- [1] a) P. Wasserscheid, T. Welton, *Ionic Liquids in Synthesis Vol. 2*, Wiley-VCH, **2007**; b) N. V. Plechkova, R. D. Rogers, K. R. Seddon, *Ionic Liquids: From Knowledge to Application*, ACS Symposium Series 1030, Washington, **2010**.
- [2] a) J. P. Hallett, T. Welton, *Chem. Rev.* **2011**, *111*, 3508–3576; b) M. J. Earle, K. R. Seddon, *Pure Appl. Chem.* **2000**, *72*, 1391–1398; c) H. Weingärtner, *Angew. Chem.* **2008**, *120*, 664–682; *Angew. Chem. Int. Ed.* **2008**, *47*, 654–670; d) J. Dupont, P. A. Z. Suarez, *Phys. Chem. Chem. Phys.* **2006**, *8*, 2441–2452; e) T. Welton, *Chem. Rev.* **1999**, *99*, 2071–2084.
- [3] a) V. I. Pârvulescu, C. Hardacre, *Chem. Rev.* **2007**, *107*, 2615–2665; b) T. Fischer, A. Sethi, T. Welton, J. Woolf, *Tetrahedron Lett.* **1999**, *40*, 793–796; c) J. S. Wilkes, *J. Mol. Catal. A* **2004**, *214*, 11–17.
- [4] Z. Ma, J. H. Yu, S. Dai, *Adv. Mater.* **2010**, *22*, 261–285.
- [5] a) H. Ohno, *Electrochemical Aspects of Ionic Liquids*, Wiley Interscience, New York, **2005**; b) S. A. Forsyth, J. M. Pringle, D. R. MacFarlane, *Aust. J. Chem.* **2004**, *57*, 113–119; c) T. Sato, G. Masuda, K. Takagi, *Electrochim. Acta* **2004**, *49*, 3603–3611; d) P. Hapiot, C. Lagrost, *Chem. Rev.* **2008**, *108*, 2238–2264.
- [6] a) T. Torimoto, T. Tsuda, K. Okazaki, S. Kuwabata, *Adv. Mater.* **2010**, *22*, 1196–1221; b) S. Tang, A. Babai, A. V. Mudring, *Angew. Chem.* **2008**, *120*, 7743–7746; *Angew. Chem. Int. Ed.* **2008**, *47*, 7631–7634.
- [7] W. R. H. Wright, E. R. Berkeley, L. R. Alden, R. T. Baker, L. G. Sneddon, *Chem. Commun.* **2011**, *47*, 3177–3179.
- [8] J. P. Hallett, C. L. Liotta, G. Ranieri, T. Welton, *J. Org. Chem.* **2009**, *74*, 1864–1868.
- [9] a) J. W. Lee, J. Y. Shin, Y. S. Chun, H. B. Jang, C. E. Song, S.-g. Lee, *Acc. Chem. Res.* **2010**, *43*, 985–994; b) L. Xu, W. Chen, J. Ross, J. Xiao, *Org. Lett.* **2001**, *3*, 295–297; c) H. Olivier-Bourbigou, L. Magna, *J. Mol. Catal. A* **2002**, *182–183*, 419–437.
- [10] R. D. Rogers, K. R. Seddon, *Science* **2003**, *302*, 792–793.
- [11] M. Khoudiakov, A. R. Parise, B. S. Brunschwig, *J. Am. Chem. Soc.* **2003**, *125*, 4637–4642.
- [12] a) S. S. Andrews, S. G. Boxer, *J. Phys. Chem. A* **2000**, *104*, 11853–11863; b) S. S. Andrews, S. G. Boxer, *J. Phys. Chem. A* **2002**, *106*, 469–477; c) S. G. Boxer, *J. Phys. Chem. B* **2009**, *113*, 2972–2983; d) G. U. Bublitz, S. G. Boxer, *Annu. Rev. Phys. Chem.* **1997**, *48*, 213–242; e) G. U. Bublitz, R. Ortiz, S. R. Marder, S. G. Boxer, *J. Am. Chem. Soc.* **1997**, *119*, 3365–3376; f) G. U. Bublitz, R. Ortiz, C. Runser, A. Fort, M. Barzoukas, S. R. Marder, S. G. Boxer, *J. Am. Chem. Soc.* **1997**, *119*, 2311–2312; g) A. Chattopadhyay, S. G. Boxer, *J. Am. Chem. Soc.* **1995**, *117*, 1449–1450; h) A. T. Fafarman, L. J. Webb, J. I. Chuang, S. G. Boxer, *J. Am. Chem. Soc.* **2006**, *128*, 13356–13357; i) E. S. Park, S. S. Andrews, R. B. Hu, S. G. Boxer, *J. Phys. Chem. B* **1999**, *103*, 9813–9817; j) E. S. Park, S. G. Boxer, *J. Phys. Chem. B* **2002**, *106*, 5800–5806; k) E. S. Park, M. R. Thomas, S. G. Boxer, *J. Am. Chem. Soc.* **2000**, *122*, 12297–12303; l) P. A. Sigala, A. T. Fafarman, P. E. Bogard, S. G. Boxer, D. Herschlag, *J. Am. Chem. Soc.* **2007**, *129*, 12104–12105; m) L. N. Silverman, M. E. Pitzer, P. O. Ankomah, S. G. Boxer, E. E. Fenlon, *J. Phys. Chem. B* **2007**, *111*, 11611–11613; n) A. J. Stafford, D. L. Ensign, L. J. Webb, *J. Phys. Chem. B* **2010**, *114*, 15331–15344; o) I. T. Suydam, C. D. Snow, V. S. Pande, S. G. Boxer, *Science* **2006**, *313*, 200–204; p) I. T. Suydam, S. G. Boxer, *Biochemistry* **2003**, *42*, 12050–12055; q) L. J. Webb, S. G. Boxer, *Biochemistry* **2008**, *47*, 1588–1598.
- [13] M. Mehata, T. Iimori, T. Yoshizawa, N. Ohta, *J. Phys. Chem. A* **2006**, *110*, 10985–10991.
- [14] a) A. T. Fafarman, S. G. Boxer, *J. Phys. Chem. B* **2010**, *114*, 13536–13544; b) A. T. Fafarman, P. A. Sigala, D. Herschlag, S. G. Boxer, *J. Am. Chem. Soc.* **2010**, *132*, 12811–12813.
- [15] Z. Getahun, C. Y. Huang, T. Wang, B. De Leon, W. F. DeGrado, F. Gai, *J. Am. Chem. Soc.* **2003**, *125*, 405–411.
- [16] T. L. Amyes, S. T. Diver, J. P. Richard, F. M. Rivas, K. Toth, *J. Am. Chem. Soc.* **2004**, *126*, 4366–4374.
- [17] a) V. C. Weiss, B. Heggen, F. Müller-Plathe, *J. Phys. Chem. C* **2010**, *114*, 3599–3608; b) F. Leroy, *J. Chem. Phys.* **2011**, *134*, 094703.
- [18] a) Y. Wang, *J. Phys. Chem. B* **2009**, *113*, 11058–11060; b) H. Zhao, R. Shi, Y. Wang, *Commun. Theor. Phys.* **2011**, *56*, 499.
- [19] a) B. L. Bhargava, R. Devane, M. L. Klein, S. Balasubramanian, *Soft Matter* **2007**, *3*, 1395–1400; b) J. N. A. Canongia Lopes, A. A. H. Pádua, *J. Phys. Chem. B* **2006**, *110*, 3330–3335; c) A. Triolo, O. Russina, H.-J. Bleif, E. D. Cola, *J. Phys. Chem. B* **2007**, *111*, 4641–4644; d) Y. Wang, W. Jiang, G. A. Voth in *Spatial Heterogeneity in Ionic Liquids*, Vol. 975 (Eds.: J. F. Brennecke, R. D. Rogers, K. R. Seddon), ACS, Washington, **2007**, pp. 272–307; e) Y. Wang, G. A. Voth, *J. Am. Chem. Soc.* **2005**, *127*, 12192–12193.
- [20] O. Russina, A. Triolo, L. Gontrani, R. Caminiti, *J. Phys. Chem. Lett.* **2012**, *3*, 27–33.

Received: April 13, 2012
Published online: August 21, 2012